Flood Extent Mapping Based on TerraSAR-X Data

Virginia Herrera Cruz, Marc Müller, Friedrichshafen & Christian Weise, München

Summary: The use of Earth observation data and techniques in the context of disaster management support has received growing importance in recent years. Due to global climate change the scientific community foresees an increase in both the intensity and frequency of extreme weather events. The high resolution, multi-polarization and multi-incidence angle capabilities of the radar satellite TerraSAR-X, its quick site access and receiving times open interesting perspectives for flood mapping and subsequent assessment of damages. Furthermore, the nearly all-weather capacity of SAR data constitutes its main advantage above optical systems for mapping of flood events. The work presented in this paper focuses on the development of an object-based classification approach for operational flood extent mapping in near-real time conditions using TerraSAR-X data. The object-based methodology is assisted by pixel-based operations and both are implemented in a solution within the eCognition software environment. The final objective is to develop a tool which can be easily used by an interpreter without the need of a profound knowledge of image processing. For this purpose an eCognition based semi-automated solution – a *Graphical User Interface* with a rule set behind – is set up. This application is tested in various scenarios and is further developed in parallel to these tests. The overall study clearly demonstrates the potential of TerraSAR-X data and object oriented methods for a rapid delineation of flood extent in an operational environment.

Zusammenfassung: *Verwendung von TerraSAR-X-Daten zur Kartierung überschwemmter Bereiche*. In den letzten Jahren hat die Anwendung von Fernerkundungstechniken sowie der Einsatz von Erdbeobachtungsdaten im Zusammenhang mit Katastrophenmanagement an Bedeutung gewonnen. Bedingt durch den globalen Klimawandel erwartet die Wissenschaftsgemeinde eine Zunahme an extremen Wetterereignissen sowohl bezüglich Ausmaß als auch Häufigkeit. Die Fähigkeit des TerraSAR-X-Satelliten, hochauflösende und multi-polarisierte Satellitenbilder unter verschiedenen Einfallswinkeln aufzunehmen sowie seine Tasking-Flexibilität und der schnelle Datenerhalt bieten erweiterte Perspektiven für die Hochwasserkartierung bzw. die Schadenabschätzung. Außerdem stellt das nahezu allwettertaugliche Aufnahmeverfahren von SAR-Daten einen bedeutenden Vorteil gegenüber optischen Daten für die Kartierung von Hochwasserereignissen dar. Die hier vorgestellten Arbeiten konzentrieren sich auf die Entwicklung eines objektbasierten Klassifikationsansatzes für das operationelle Kartieren von Hochwasser unter nahe Echtzeit-Bedingung und unter Verwendung von TerraSAR-X-Daten. Die objektbasierte Methode wird unterstützt durch eine pixelbasierte Methode, beide Ansätze sind in einer eCognition-Softwareumgebung implementiert. Ziel ist die Erstellung eines Software-Werkzeuges, das relativ einfach und ohne fundierte Kenntnisse der Bildbearbeitung eingesetzt werden kann. Zu diesem Zwecke wurde eine auf eCognition basierende semi-automatische Lösung entwickelt, die eine graphische Benutzeroberfläche inklusive Regelsatz im Hintergrund als wesentlichen Bestandteil hat. Diese Lösung wurde in verschiedenen Szenarien getestet und parallel dazu weiterentwickelt. Insgesamt zeigen die Ergebnisse deutlich das Potential von TerraSAR-X-Daten und objektorientierten Methoden für eine schnelle Kartierung der Hochwasserausdehnung unter operationellen Bedingungen.

1 Introduction

Flood is one of the most widespread natural disasters and the one which affects the highest number of people in average (CRED 2009). It regularly causes large numbers of casualties with increasing economic loss. Annually flood events result in estimates of up to 25,000 deaths worldwide, extensive homelessness, disaster-induced disease, crop and livestock damage and other serious harm (UNU 2010). Even the most advanced nations are severely affected: The seasonal floods of the Mississippi River have averaged 25 deaths annually since the 1980s (ibid.). In Europe, the 2002 floods killed roughly 100 people, affected 450,000 people and left $ 20 billion in damages (ibid.). Already in the first half of 2010, floods caused by the storm Xynthia have affected all Atlantic countries from Portugal to Germany, hitting especially France. Also, in March 2010 the continuing rain was inundating the South of Spain, leaving hundreds of people homeless. Only two to three month later heavy rains caused floods in Poland, Hungary, Slovakia and the Czech Republic – let alone the devastating flood events in China and above all in Pakistan in August of 2010. The latter affected almost 14.5 million people with an official death toll risen to 1,384 and with 1,680 people reported as injured. Over 722,000 houses have been either damaged or destroyed (UN-SPIDER 2010). Consequently, disaster management is of particular humanitarian, social, economic, and political interest. It involves assessments of vulnerability and risk, the monitoring of hazard prone zones, the planning and management of rescue operations and post disaster damage assessment to be finally better prepared for the next time of a disastrous event.

Using remote sensing data allows for mapping inundated areas for a more accurate assessment of the disaster extent – especially for areas difficult to access – and for a more large-scale and cost-effective way than ground observation (WAISURASINGHA et al. 2008, OKAMOTO et al. 1998). Remote sensing is also an important information source for the calibration of hydrological models which are used, e. g., in forecasting (ZWENZNER & VOIGT 2009). Optical data as well as radar data – both airborne

(e. g., RAMESH et al. 2010) and space-borne – has been used for this purpose. Using optical data (especially its red to SWIR spectrum) is often referred to as a most straightforward way to extract flood extent from Earth observation data (JI et al. 2009). HUANG et al. (2009) – analysing Spot-5 data – and IRIMESCU et al. (2010) – using MODIS TERRA and AQUA data – are among the related works. Other satellites used are, e. g., Landsat and the Advanced Very High Resolution Radiometer (JI et al. 2009). IRIMESCU et al. (2010) propose the use of Normalised Difference Vegetation Index (NDVI) for water detection while JI et al. (2009) defends when possible the use of NDWI calculated from green-SWIR / green+SWIR. Nevertheless, as flooding is often associated with extreme weather events, optical data acquisition encounters limitations due to cloud coverage. Contrarily, radar data presents the advantage of its near all weather operating capability allowing to acquire imagery of affected areas also during night time. Therefore radar is seen as the only secure alternative for mapping flood events in its peak (SCHUMANN et al. 2009). For a long time its limited resolution has been seen as a hinder for its use in mapping of flood events. In 2006 SCHUMANN et al. (2006) reported SAR data as having medium spatial resolution, often limited to single frequency, difficult to georectify accurately and geometrically and radiometrically distorted. But the new SAR satellites generation overcome these limitations by providing a wide catalogue of resolutions (down to 1 meter) and swaths with a very appropriate relation for flood evaluation. Discussion about the appropriate spatial resolution for flood mapping can be found in SCHUMANN et al. (2009). Furthermore, today's SAR data – and especially TerraSAR-X data – is highly precise in terms of geocoding, positional accuracy and absolute radiometric calibration (AGER & BRESNAHAN 2009).

The examples presented here focus on three flood events of high intensities that occurred in June 2008 in a highly populated area of the USA and in February 2009 and April 2009 in two savannah areas of Australia and Namibia, respectively.

The first area of interest is located close to the St. Louis County (Missouri). The flood

event that occurred from May to August 2008 was caused by heavy rains. It affected high populated areas of the States of Illinois, Indiana, Iowa, Michigan, Minnesota, Missouri, and Wisconsin.

The second area is the Gulf Country region in North Queensland. It is a large savannah area with a monsoonal climate characterised by the alteration of dry winters and wet summers. It has a well known dynamic of flood events. Populations in the area are used to have three to four weeks of isolation during the wet season. Nevertheless, at the beginning of 2009, the unexpected volume of water kept the two towns of the area much longer isolated.

Finally, the Caprivi region is a narrow strip of land compressed between the arms of the Zambezi and the Kwando rivers and bordering with the countries Zambia, Botswana and Zimbabwe. The area is the wettest of Namibia, with a seasonal tropical climate with the rainy season lasting from December to March.

2   SAR Based Flood Extent Mapping

In this paper main emphasis is put on the development of a SAR-based flood mapping workflow suited for an operational implementation. In this domain quite a lot of research has been done in recent years (MARTINIS et al. 2009). Often used is the thresholding of the image histogram (MARTINIS et al. 2009, GEBHARDT et al. 2008, HENRY et al. 2006, SCHUMANN et al. 2006) or of an arithmetic image (ratio or difference usually, BRAKENRIDGE et al. 2003) with different methods of interactive or automatic detection of the threshold values. Thresholding is a simple and resources economical method, but when applying it to pixels it requires a previous speckle filtering and again post-processing filtering and it is only effective in well contrasted images (MARTINIS et al. 2009).

Segmentation approaches play then an important role. The mapping process benefits, this way, not only from the absence of the salt and pepper effect, but also from the textural and contextual information contained in the objects. Sophisticated methods as Artificial Neural Networks (KUSSUL et al. 2008) or Active Contour Models – in its statistical variation (HORRITT et al. 2001, MASON et al. 2010) or in its geometric variant (HUANG et al. 2005) so called level-sets – have been applied to segment SAR data in the context of flood mapping both for whole scenes and region-based (SILVEIRA & HELENO 2009). But Active Contour Models require enormous data preparation which today prevents their application for near real time mapping. A common approach for segmentation, more simple to apply are algorithms using the *Fractal Net Evolution Approach* (FNEA), commercially introduced by BAATZ & SCHÄPE (1999) and implemented in the eCognition software. NEUBERT et al. (2008) and MEINEL & NEUBERT (2004) show in an extensive review and comparison of segmentation methods best performances for the FNEA.

To profit from the simplicity of thresholding and the additional information saved in the pixel objects and the description power of the decision trees, different combined approaches could be considered. MARTINIS et al. (2009) for example combine a histogram thresholding approach and a segmentation based classification for flood detection in high resolution TerraSAR-X data. The threshold is automatically calculated based in local thresholding analysis of selected areas or splits. The threshold is afterwards integrated into a multi-scale segmentation process. They proved the better performance of object-based thresholding over pixel-based one. TOWNSEND (2001) and PIERDICCA et al. (2009) combine multiple thresholds with decision trees. Another possible combination is the supervised and unsupervised method: For instance, at the Center for Satellite Based Crisis Information of the German Aerospace Center an unsupervised clustering algorithm is applied to images enhanced by local image statistics (minimum / maximum, mean and variance) followed by interactively identification of water clusters (HAHMANN et al. 2008).

Considering multi-temporal analysis as superior to single data approaches (HAHMANN et al. 2008) change detection methods to detect variations of backscatter or on the coherence among SAR image pairs (BONI et al. 2007, PIERDICCA et al. 2008) or by using ratios (AN-

DREOLI & YESOU 2007) are also widely investigated. One advantage of those methods is that they profit by comparison possibilities in many cases of uncertainties. The disadvantage is that these methods require much data preparation (ANDREOLI & YESOU 2007) and strongly depend on available pre-event data which is not always at hand in a real emergency situation.

Also, real emergency events require simple tools which can provide a rapid and accurate overview of the situation. Such a tool should be time-effective, reliable, robust and flexible enough to adapt to the circumstances in relation to data and staff available. This kind of a simplified tool also offers the benefit directly to be used by local operators. For all these reasons the creation of a robust rule set and the creation of a user interface for operators having local knowledge but not being remote sensing experts was the guiding idea during the development of the method right from the beginning of the DeSecure project (DESECURE 2010).

The mapping of water with SAR data is based on the specular behaviour of the microwave signal when encountering a smooth surface. For instance, in the case of calm water, the SAR signal is scattered away and the surface appears dark in the satellite image. However, in case of a flood event, when extreme winds and rain occur at the time of image acquisition, the induced changes in the smooth surface of the water can increase the intensity of the response signal and produce artefacts which will complicate a straightforward classification of the flooded surface (KUSSUL et al. 2008). Further difficulties are flooded vegetation and / or man-made structures. Different structures poking out of the water can produce a enhancement of the signal due to a double bounce effect in the different SAR bands. This effect depends on the relation between the size and spacing of the structures and the chosen wavelength. As an example, changes from flood to not flooded in forested areas can be observed in C-band (HAHMANN et al. 2008) and with L-band (TOWNSEND 2001), because the signal is able to penetrate the forest canopy. Concerning X-band the shorter wavelength does not allow the penetration of the forest canopy (HAHMANN et al. 2008). For further de-

tails on the different SAR signal interactions with the Earth's surface it is referred to Raney in HENDERSON & LEWIS (1998).

The work presented here focuses on the development of a semi-automated procedure for flood extent mapping under near-real time (NRT) conditions. NRT is here understood as a combination of delivering TerraSAR-X images to the operator within 2 hours after image acquisition plus producing and delivering the flood extent map to the user within 2 hours on top.

The whole flood mapping procedure is implemented within the eCognition software suite and developed in the Cognition Network Language (CNL). CNL is an object-based procedural computer language which is specially designed to enable the analysis of complex, interactive, context-dependent image analysis tasks, like flood mapping. Each language element representing the dynamic of the analysis is called "process" and organized in a process tree hierarchy (rule set). Especially interactive processes allow interactions with users in an image analysis workflow. The execution environment of the software suite uses a workspace concept in which the user of a workflow may process many images offline and – if needed – in parallel on a computer cluster. It is thus possible to give a step-wise structure to the flood mapping analysis, to separate modules with different degrees of automation in the overall workflow and to analyze images in a production mode.

The outputs of the tests using eCognition confirmed the potential of TerraSAR-X data and the object-oriented methods for a rapid de-
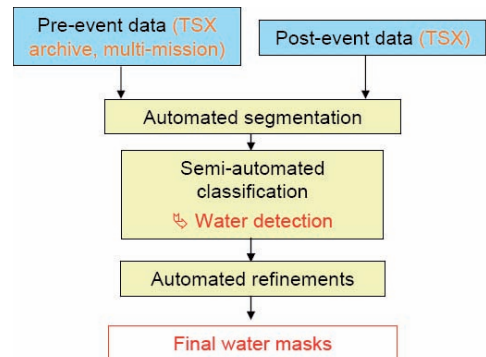

Fig. 1: Flood mapping – general workflow.

lineation of flood extent in an operational environment. The resulting mapping chain is completed by building a Graphical User Interface (GUI). Three modules sequentially activated are distinguished in the developed rules system: Segmentation with automated AoI (Area of Interest) selection, semi-automated extraction of water masks (classification) and automated final refinement (Fig. 1).

After introducing the satellite data used here including a description of the data characteristics and the pre-processing steps (Section 3) each of the three modules is explained separately in the Sections 4–6.

3   Data Set Selection and Preparation

TerraSAR-X is a German radar satellite operating in X-Band (9.65 Gigahertz). In the standard operating mode image data can be acquired in three different imaging modes: ScanSAR, StripMap and SpotLight modes which differ in their spatial coverage and spatial resolution. The ScanSAR mode provides the largest possible coverage with a single scene of 100 km (range) × 150 km (azimuth, extension up to 1,650 km possible) and a corresponding ground resolution of 18 m. StripMap scenes cover a 30 km wide swath with a typical length of 50 km (also extendable to 1,650 km), the ground resolution improves to 3 m. Finally, the SpotLight mode allows the observation of relatively small areas (10 × 10 km²) at up to 1 m resolution.

The high resolution, multi-polarization and multi-incidence angle capabilities of TerraS-AR-X data acquisition open very interesting perspectives for flood mapping and damage assessment. Further, the system capabilities of TerraSAR-X render the satellite as a valuable imagery source for disaster management and site monitoring, e. g., due to the satellite's quick site access time of 2.5 days to any point on Earth at 95 % probability.

The programming of TerraSAR-X acquisitions for the affected regions requires a number of decisions regarding acquisition parameters (for a detailed description of products and parameters see FRITZ & EINEDER 2009). The selection of the best suitable acquisition mode is based on the size of the area affected. Strip-Map was chosen to cover the area selected for the Mississippi event while ScanSAR scenes were acquired for the Gulf Country and the Caprivi region, respectively. Additionally, SpotLight data of Caprivi were also used for a more detailed mapping. Compared to VV polarization, the HH polarized backscatter coefficient generally presents higher contrast between water and land surfaces (HENRY et al. 2006). The use of dual polarization data results in a reduced coverage and resolution, which needs to be traded off against the increased information content. Here, HH polarisation was used for all areas of the study. Shallow incidence angles are preferred for flood mapping as steep incidence angles result in stronger backscatter for open water and reduce the contrast to land surfaces. In an emergency, however, acquiring the first possible scene of the area affected clearly takes priority over considerations on the choice of a proper incidence angle. For mapping the flood extent geocoded data sets are required (EEC products). Concerning the resolution mode, preference is given to RE products (radiometrically enhanced) as they already comprise a speckle reduction and are therefore more suited to segmentation processing.

In parallel to the acquisition planning, an archive search on existing pre-event and auxiliary data is required. TerraSAR-X data are preferred as pre-event data, since scenes acquired by the same sensor can be directly compared to each other. However, if no TerraSAR-X pre-event acquisitions are available, data from any other available source are used (e. g., optical, airborne data). In case of the Mississippi flooding, no TerraSAR-X archive data of the region was available. Thus, a Landsat 7 image was deployed for pre-event information. Additionally, approximately four months after the flood a new TerraSAR-X StripMap scene of the area was acquired and used as pre-event data, to simulate a real scenario for which TerraSAR-X archive data would be available. Also in Namibia, data of the flood recession period had to be used as simulated pre-event data. However, by the time the floods in Queensland occurred, the TerraSAR-X Background Mission was able to supply pre-event data from archive for that

Tab. 1: Mississippi area.

Sensor	Centre (lon/lat)	Imaging Mode	Product	Acquisition date
TerraSAR-X	−90.75° / 38.96°	SM	EEC/RE	23 June 2008
	−90.61° / 39.15°	SM	EEC/RE	17 October 2008
Landsat7	39.3°/ 90.7°	-	-	10 January 2008

Tab. 2: Gulf Country area.

Sensor	Centre (lon/lat)	Imaging Mode	Product	Acquisition date
TerraSAR-X	−17.15°/ 141.00°	SC	EEC/RE	3 June 2008
	−17.25/ 141.23°	SC	EEC/RE	11 February 2009

Tab. 3: Caprivi area.

Sensor	Centre (lon/lat)	Imaging Mode	Product	Acquisition date
TerraSAR-X TerraSAR-X	24.76°/−17.68°	SC	EEC/RE	11 April 2009
	24.72°/−17.59°	SC	EEC/RE	1 September 2009
	24.78°/−17.88°	SL	EEC/RE	6 April 2009
	24.71°/−17.92°	SL	EEC/RE	7 September 2009

area, and therefore a complete ScanSAR data set (pre and post event) could be analysed in that case. Detailed information on the image parameters is shown in Tabs. 1–3.

Auxiliary data sets are also of great importance. Any supplementary information about the test site support and accelerate the event interpretation. It also reduces the effort for the refinement step which is later described. In addition to the image data sets, a visual interpretation of the environmental conditions was performed for the Australian flood event. This interpretation map, chiefly based on manual work, was used as reference.

4 Automated Segmentation

Segmentation is the process of completely partitioning a scene (e. g., a remote sensing image) into non-overlapping regions (segments) in scene space (e. g., image space SCHIEWE 2002), based on homogeneity and heterogeneity criteria, respectively (HARALICK & SHAPIRO 1985 in NEUBERT et al. 2006). In the

object-oriented classification, the final aim of the segmentation is to delineate the meaningful regions which represent the objects that need to be classified. Despite the popularity of segmentation processes for remote sensing images in the last years, segmentation is by no means a new field of research. On the contrary, segmentation was already in the 1970's a topic of interest (cf. KETTIG & LANDGREBE 1976). And so far, about one thousand kinds of segmentation approaches have already been developed (CHEN & LUO 2003) within disciplines like artificial intelligence, signal processing, computer vision etc. with successful applications in medicine, telecommunications, engineering or neuro-informatics (SCHIEWE et al. 2001). There is a high variety of segmentation algorithms already available for remote sensing images. A good review and comparison can be found in NEUBERT et al. (2008) and MEINEL & NEUBERT (2004).

Referring back to Section 2, *FNEA* is one of the most commonly used approaches. It is a bottom-up region-growing technique starting with one-pixel objects. In many subsequent steps smaller image objects are merged into

larger ones. The growing decision is based on local homogeneity criteria describing the similarity of adjacent image objects in terms of size, distance, texture, spectral similarity and form. The scale at which this segmentation is done can and has to be chosen in relation to the characteristics of the data set and the objective of the work. The aim of the segmentation is to delineate the meaningful regions which represent the objects that will be classified. For this reason it is mandatory for the quality of the further classification step that the borders of the water bodies (permanent or not) are clearly highlighted.

The segmentation module of the process developed here is a rule set for automated analysis which basically combines cycles of MRS and classification and is assisted by other more simple segmentations not based on the image content (chessboard segmentation). To allow the processing of large data sets the rule set included the tiling, parallel processing and final stitching of the region. In order to accelerate the segmentation, which is the most time consuming process of the overall flood mapping processing chain, only regions potentially containing water are automatically selected and segmented. Thus, the amount of segments (objects) and the respective processing time is drastically reduced. The result is an automated and target-centred segmentation "image" in which the information of both dates, pre and post event is taken into account. The process

can be batched to analyse as many images as necessary.

The activation of the automated segmentation step is initiated with an automated revision of the project parameters for the number of layers and the calculation of scene statistics (mean, standard deviation and extreme pixel values). Then – after tiling the image – the parallel processing begins for each tile with a chessboard segmentation. By this means the whole tile is segmented into squares of 60×60 pixels. Based on the scene statistics previously calculated and on empirical analysis of a large collection of SAR data, different threshold values are identified for units not containing water. Those values will be included as previous condition for the segmentation. If the square object in question is within this threshold or in contact to an object which is in it, it will be segmented.

The segmentation of the units containing water is then made using the MRS algorithm. Considering objects not as a static unit, but as a dynamic concept in which objects grow, shrink, and become re-segmented and smoothed etc., there exists a wide range of scale parameters which could fit the segmentation purposes here. Hence, an ideal parameter set for a perfect segmentation can never be selected.

Pragmatically, the necessary parameter adjustments depend on the size, shape and backscatter of the expected objects and the speci-
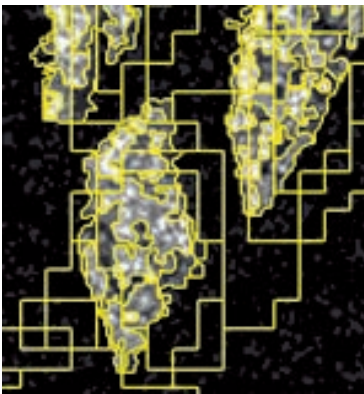
Fig. 2: MRS result using Landsat 7 and TerraSAR-X data – Overlaid on **TerraSAR-X** post-event scene.
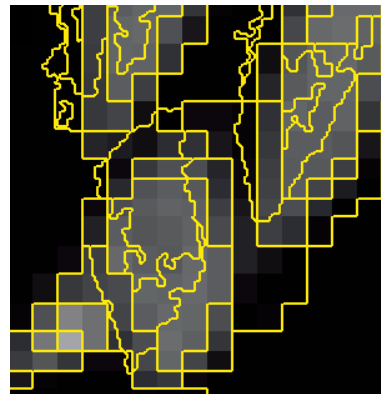
Fig. 3: MRS result using Landsat 7 and TerraSAR-X data – Overlaid on **Landsat 7** pre-event scene.

fied Minimum Mapping Unit (MMU). In this study – depending on the availability of one or two scenes as input data – a mono-temporal segmentation or a bi-temporal segmentation, respectively, has been automatically performed. Both processes will produce only one segmentation layer, but for the bi-temporal segmentation a segmentation of the pre-event dataset is produced inside the segments of the post-event data set. Finally, all tiles are stitched together. A re-segmentation of the tile borders is then conducted to harmonize the segments in the whole scene and to avoid false objects created by the tiles' borders.

Figs. 2 and 3 display an example of the segments obtained using a combination of TerraSAR-X and Landsat data for the Mississippi scenario. The same segments are displayed once over the TerraSAR-X post-event scene and once over the Landsat 7 scene. As it can be seen the automated segmentation process uses information of both scenes. When comparing these segmentation results to those obtained using only TerraSAR-X data the object shapes differ between the two scenarios due to the different resolution of the two pre-event layers (3 m, TerraSAR-X image vs. 30 m [resampled to 3 m], Landsat 7 image) and the different nature of radar and optical imaging techniques. Specifically, the speckle of the SAR data strongly influences the object shapes and sizes.

5 Semi-automated Extraction of Water Mask (Classification)

Unlike pixel-based techniques which only use the pixel values, the object-based techniques can also use texture, shape and context information of a scene. The optimal features, i. e., measurable properties of the segments, for water detection are identified and constitute the basis for the "water" / "non water" classification of the pre-event and post-event scenes.

The similar spatial behaviour of water in SAR images and in the NIR channel of optical data is used here as common ground for a flood mapping workflow considering not only TerraSAR-X data, but also optical archive data: In optical images, water absorbs most of the incident radiation and therefore appears dark in colour-infrared images. The characteristic spectral reflectance curve shows a reduction of intensity with increasing wavelength. In the near infrared the reflectance of deep, clear water is virtually zero, for this reason the channel 4 of Landsat 7 is used for the discrimination of water / non-water; in case of SAR X-band, under low to moderate wind conditions, backscatter from water surfaces is low. Thus, a water body appears dark compared to the backscatter of other land cover features; based on this water surface behaviour, a rule-based classification system with tuneable variables and a user-friendly interface is constructed for the effective extraction of the water extent.

The first classification step is based on an object-based thresholding of the intensity values, controlled by texture, shape and context features. A tool supports the operator allowing him to manipulate the different features so that the water mask extent can be changed online. However, the resulting water cover is not always perfect, as can be seen in Fig. 4, which shows the permanent water body extracted using channel 4 of the Landsat scene (a) and the TerraSAR-X scene (b), respectively. Main discrepancies in these two water masks result from the diverse image resolutions and from the different acquisition dates. It can be noticed that in the two cases areas affected by shadows are classified as water since they present a low reflectivity. These errors that appear in more in the Landsat classification are corrected with further widgets that can be optionally used. Two types of corrections or interactive refinements are implemented with those widgets. The first one is an objects-based reclassification of the "water" segments, based on the previously defined water class. The second one is the pixel-based thresholding of the water borders and neighbouring objects. As in some occasions a certain water course is interrupted because few water pixels dropped in a mainly non-water polygon. Subsequent to the pixel-based correction the water course will be connected again.

For the post-event data the semi-automated extraction of the water mask is based on the same methodology. The obtained results are shown again in Fig. 4 for the Mississippi River case (c and d). The water masks look similar
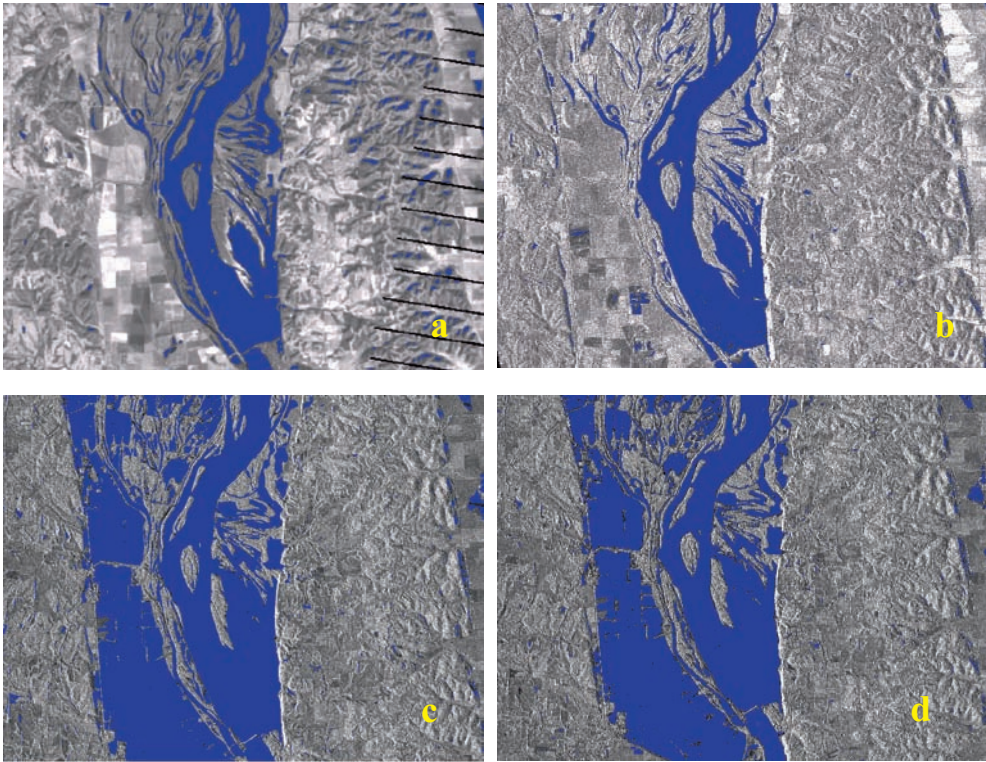
Fig. 4: a) Landsat 7-based *pre-event* water mask b) TerraSAR-X-based *pre-event* water mask c) TerraSAR-X-based *post-event* water mask d) Permanent water / flood mask derived from the combination of Landsat 7 and TerraSAR-X data.
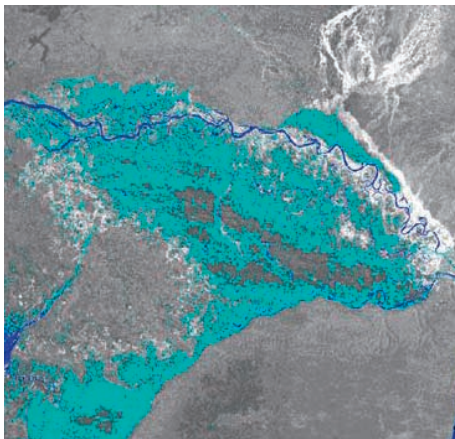
Fig. 5: Intermediate step – result of the semi-automated classification (blue: permanent water body, cyan: flooded area).
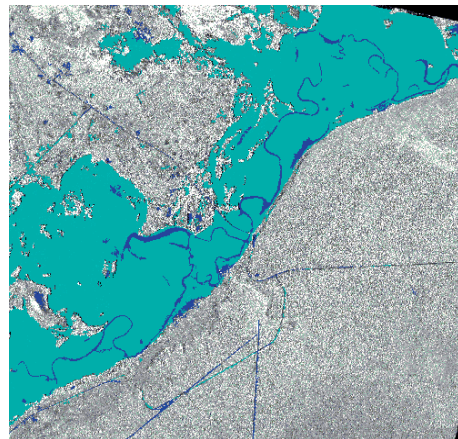
Fig. 6: Intermediate step – result of the semi-automated classification (colours: see left).

despite the fact that two different layers were used as pre-event data for the original segmentation. It is worth mentioning that the selection of the pre-event layer had a direct impact on the shape and size of the objects and on the specific value needed for the features to be selected within the classification process.

The need for refinements of the water masks typically depends on the relief and on the environmental conditions. For example, wind has a particular influence on SAR-based classification results as higher wind speeds could result in larger errors. In the Caprivi scenario, the strong winds affecting the ScanSAR scene prevented the detection of the whole mass of water (Fig. 5). In comparison, the SpotLight scene (Fig. 6), recorded at a different date and with a shallower angle shows a very clear distinction of water and therefore needs nearly no refinement steps. Worth mentioning are also the double-bounce effect that can be observed to the sides of the rivers (Fig. 5).

6   Automated Refinements

The final step in the flood mask production is the generation of two water masks in order to separate the flooded areas from the permanent water bodies such as rivers, lakes and ponds.

The automated refinement step consists in the improvement of the classifications made on the pre-event and post-event scenes. It includes the automated extraction of the flood and permanent water masks as well as the application of final refinements such as smoothing and minimum mapping filters. A final MMU is also defined depending on the quantity of detail desired in the final water mask and the precision of the final map, respectively. Finally, the borders of the polygons are smoothed using growing and shrinking pixel based algorithms.

The results obtained for the Australia case are very satisfying. Fig. 7 shows a detail of the area considered for the analysis. A reference map (Fig. 8) was manually delineated for part
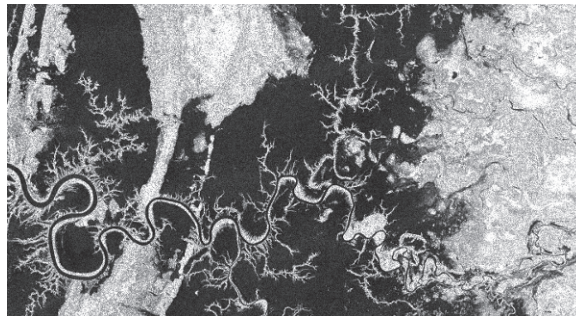
Fig. 7: Detail of ScanSAR post-event scene over the Gulf Country affected area. Low backscattering of the radar signal (dark) indicates permanent water and flooded areas, respectively.
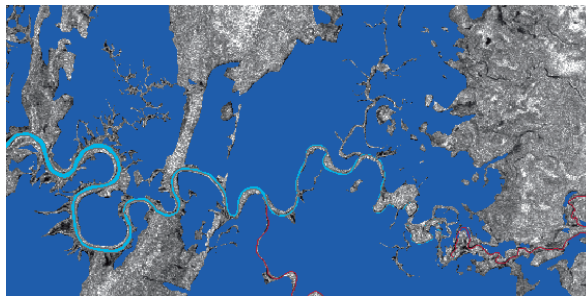
Fig. 8: Manually delineated water extent map (reference), Gulf Country (cyan: permanent water body, blue: flooded area), superimposed on ScanSAR post-event scene (colours in the background due to display).
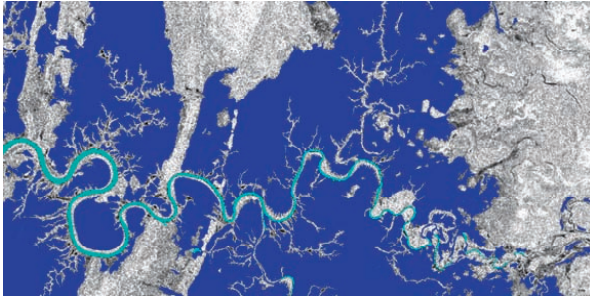
Fig. 9: Final flood mask product from the semi-automated procedure, Gulf Country (colours and background as above).

of the ScanSAR image. This map allowed a preliminary qualitative evaluation of the results (Fig.9) of the developed flood mapping processing chain. Further qualitative and quantitative evaluations are currently under way.

It is worth mentioning that the manual delineation required more time for a third of the total scene than time needed by the semi-automated process for the whole scene. This means that even if no further process was implemented for the correction of the shadows in flood plain areas, it could be assumed that deselecting areas of shadows by manual editing tools might be still more time-effective than visual interpretation.

7 Conclusion and Outlook

This paper gives an overview of the development and implementation of a TerraSAR-X based semi-automated workflow for flood extent mapping performed in the framework of the DeSecure project.

For this purpose we combined a series of existing techniques for pixel- and object-based analysis to produce a user friendly tool for flood mapping. The developed semi-automated workflow was tested in a variety of scenarios and a preliminary validation of the results has been made confronting them with flood extent maps generated manually by visual interpretation. Finally, the workflow was implemented into a pre-operational test using two different TerraSAR-X products: A bi-temporal ScanSAR data set and a bi-temporal SpotLight data set.

Altogether, TerraSAR data demonstrated its high capacity for the mapping of flood events. Furthermore, the high resolution, the multi-polarization and multi-incidence angle capability of TerraSAR-X, its quick site access and receiving times open very interesting perspectives for flood mapping and the assessment of damages after a natural disaster. Concerning an automation of mapping processes, the degree to which it can be applied is directly related to the quality of the received SAR signal in the available TerraSAR-X images for the respective flood events. Strong wind or rain and some landscape conditions might lead to certain noise or other effects which produce an atypical backscatter signal of water. This effect is intensified by a shallow incidence angle of the acquired scene. As near-real time conditions for flood mapping are also addressed, it is not possible to change the environmental condition if they are not favourable. However, the image acquisition capabilities (e. g., combining descending and ascending orbits) and the quick tasking of the satellite can provide within relatively short time more images to counteract such disturbances.

Nevertheless, object-based methods – which allow the use of context information – and the stepwise approach with its different levels of automation and possibility for parameter tuning showed to be rather adjustable to these circumstances.

The ScanSAR post event scene for the Namibia scenario was a good example of unfavourable conditions: On the one hand low incidence angle and wind, on the other hand water covered areas under vegetation provoking double-bounce effects changing the typi-

cal low backscattering characteristic of water. As a consequence for the mapping the ScanSAR-based map required more post-processing than the SpotLight-based one, which only required minor corrections.

In terms of workflow the main findings and framework conditions to be put here can be summarised as follows:

Large images were successfully processed ($30 \times 50\,km^2$ [StripMap], $100 \times 150\,km^2$ [ScanSAR]) and the TerraSAR-X RE products could be used without previous pre-processing or need of speckle filtering:

The adaptability and flexibility of the workflow was demonstrated applying it to satellite scenes representing different environmental conditions. Concerning the mapping chain's robustness it has been tested using different TerraSAR-X imaging modes and, as in case of the Mississippi River flooding, different sensors (TerraSAR-X data [3 m res], Landsat 7 ETM+ [30 m res]). Nevertheless, to draw conclusions about the rule set's performance using optical data, further tests are required. Regarding the result's uncertainties caused by strong winds and / or rain during image acquisition, additional manual editing may be required while in some special cases the meteorological conditions may not allow the application of the rule set in all. However, in order to minimise wind and rain effects in the satellite image, the incidence angle of the TerraSAR-X data acquisition should be as shallow as possible. As to the homogeneity level of the segments this can be adjusted by the operator, reflecting the system's adaptation possibilities, especially when the environmental conditions during image acquisition are not favourable (inundations in densely wooded areas are unfavourable but have not yet been analysed). Under favourable conditions though, the manual editing is minimised but cannot be eliminated completely.

The enhancements of the semi-automated system as presented here towards a multi-mission suited system, has several advantages for a NRT damage assessment: Highly accurate flood extents could be delineated even if no TerraSAR-X pre-event data are available. And, the revisit time over the affected region is increased by the use of multi source remote sensing data which is an important factor when processes such as rising or declining water levels should be monitored. Nevertheless, one should not forget the additional effort required for co-registration when working with different sensors.

Regarding the validation of the flood mapping for the Australian Gulf Country test site it has been noticed that, first of all, the processing of the whole scene with the developed procedure required approximately less than 5 % of the working time than the manual delineation of the flood extent. Secondly, the flood delineation results of either method were identical. Finally, this comparison has also demonstrated the effectiveness of the workflow: The mask generated with the semi-automated process shows a level of detail that an interpreter by means of digitising is not able to reach in reasonable time. Concerning further qualitative and quantitative evaluations of the results the analysis has only recently been initiated and could not be completed within the term of the DeSecure project. Nor was it possible to perform any field work or to collect field data and / or additional reference data.

Using SpotLight scenes showed to be the ideal condition for an automated mapping of a flood event. It was concluded that within one to two hours after image availability at the operator it is possible to produce a rapid flood extent map (best case scenario for two TerraSAR-X SpotLight acquisitions or subsets in case of larger TerraSAR-X data sets). From this point in time, additional time needs to be considered depending on the need of pre-processing non TerraSAR-X data, the number of pixels to processed, the level of detail required, the level of accuracy and smoothness required for the delineation of the boundary between "water" and "no water" and the level of uncertainty given by the environmental conditions during image acquisitions.

References

Ager, T.P. & Bresnahan, P.C., 2009: Geometric precision in space radar imaging: Results from TerraSAR-X – ASPRS Annual Conference: on CD.

Andreoli, R. & Yesou, H., 2007: Change detection analysis dedicated to flood monitoring using Envisat wide swath mode data. – Envisat symposium: on CD.

BAATZ, M. & SCHÄPE, A., 1999: Multiresolution segmentation – an optimization approach for high quality multiscale image segmentation. – Angewandte Geographische Informationsverarbeitung.

BONI, G., CASTELLI, F., FERRARIS, L., PIERDICCA, N., SERPICO, S. & SICCARDI, F., 2007: High resolution COSMO/SkyMed SAR data analysis for civil protection from flooding events. – IGARSS: on CD.

BRAKENRIDGE, G.R., ANDERSON, E., NGHIEM, S.V., CAQUARD, S. & SHABANEH, T., 2003: Flood warnings, flood disaster assessments, and flood hazard reduction: the roles of orbital remote sensing. – 30th International Symposium on Remote Sensing of the Environment: on CD.

CHEN, Q. & LUO, J., 2003: A geostatistic based segmentation approach for remotely sensed images. – www.definiens.de.

CRED (Centre for Research on the Epidemiology), 2009: Disasters in numbers. – New release. www.unisdr.org/preventionweb/files/12470_2009disasterfigures.pdf (15th June 2010).

DESECURE, 2010: DeSecure project homepage. – www.desecure.info/intro_de.html (15th June 2010).

GEBHARDT, S., KÜNZER, C., WEHRMANN, T., GSTAIGER, V., HUTH, J., SCHETTLER, H. & SCHMIDT, M., 2008: The WISDOM Project – A water-related Information System for the Mekong Delta, Vietnam: first results of remote sensing. – World water congress: on CD.

FRITZ, T. & EINEDER, M. (Eds.), 2009: TerraSAR-X Ground Segment, Basic Product Specification Document, Issue 1.6.

HAHMANN, T., ROTH, A., MARTINIS S., TWELE, A. & GRUBER, A., 2008: Automatic extraction of water bodies from TerraSAR-X data. – IGARSS 2008: 103–106.

HARALICK, R. & SHAPIRO, L., 1985: Image segmentation techniques. – Computer Vision, Graphics, and Image Processing 29: 100–132.

HENDERSON, F.M. & LEWIS, A.J. (Eds.), 1998: Principles and applications of imaging radar. – Manual of Remote Sensing 2, John Wiley & Sons, Inc..

HENRY, J., CHASTANET, P., FELLAH, K. & DESNOS, Y., 2006: Envisat multipolarized ASAR data for flood mapping. – International Journal of Remote Sensing 27 (10): 1921–1929.

HORRITT, M.S., MASON, D.C. & LUCKMAN, A.J., 2001: Flood boundary delineation from Synthetic Aperture Radar imagery using statistical active contour model. – International Journal of Remote Sensing 22 (13): 2489–2507.

HUANG, B., LI, H. & HUANG, X., 2005: A level set method for oil slick segmentation in SAR images. – International Journal of Remote Sensing 26 (6): 1145–1156.

HUANG, M., GONG, J., SHI, Z. & ZHANG, L., 2009: River bed identification for check-dam engineering using SPOT-5 image in the HongShiMao watershed of the Loess Plateu, China. – International Journal of Remote Sensing 30 (8): 1853–1865.

IRIMESCU, A., CRACIUNESCU, V., STANCALIE, G. & NERTAN, A., 2010: Remote sensing and GIS techniques for flood monitoring and damage assessment. – Study case in Romania, BALWOIDS 2010, Ohrid, Republic of Macedonia: on CD.

JI, L., ZHANG, L. & WYLIE, B., 2009: Analysis of dynamic thresholds for the Normalized Difference Water Index. – Photogrammetric Engineering and Remote Sensing 75 (11): 1307–1317.

KETTIG, R.L. & LANDGREBE, D.A., 1976: Classification of Multispectral Image Data by Extraction and Classification of Homogeneous Objects. – IEEE Transactions on Geoscience Electronics 14 (1): 19–26.

KUSSUL, N., SHELESTOV, A. & SKAKUN, S., 2008: Grid system for flood extraction from satellite images. – Earth Science Informatics 1: 105–117.

MARTINIS, S., TWELE, A. & VOIGT, S., 2009: Towards operational near real-time flood detection using a split-based automatic thresholding procedure on high resolution TerraSAR-X data. – Natural Hazards and Earth System Science 9: 303–314.

MASON, D.C., SPECK, R., DEVEREUX, B., SCHUMANN, G.J.P., NEAL, J.C. & BATES, P., 2010: Flood detection in urban areas using TerraSAR-X. – IEEE Transactions on Geoscience and Remote Sensing 48 (2): 882–894.

MEINEL, G. & NEUBERT, M., 2004: A Comparison of segmentation programs for high resolution remote sensing data. – XXth ISPRS Congress: on CD.

NEUBERT, M., HEROLD, H. & MEINEL, G., 2008: Assessment of remote sensing image segmentation quality. – GEOBIA: on CD.

OKAMOTO, K., YAMAKAWA, S. & KAWASHIWA, H., 1998: Estimation of flood damage to rice production in North Korea in 1995. – International Journal of Remote Sensing 19: 365–271.

PIERDICCA, N., CHINI, M., PULVIRENTI, L. & MACINA, F., 2008: Integrating physical and topographic information into a fuzzy scheme to map flooded area by SAR. – Sensors 8: 4151–4164.

RAMESH, A., GLADE, T., KAPPES, M. & MALET, J.P., 2010: Delineation of Flood inundated areas using aereal photpinterpretation and GIS-based hydrological modelling – an application in Barcelonnette, France. – Geophysical Research Abstracts 12, EGU General Assembly 2010: on CD.

Schiewe, J., Tufte, G.L. & Ehlers, M., 2001: Potential and problems of multi-scale segmentation methods in remote sensing. – GIS – Geographische Informationssysteme **6:** 34–39.

Schiewe, J., 2002: Segmentation of High-Resolution Remotely Sensed Data – Concepts, Applications and Problems. – International Archives of Photogrammetry Remote Sensing and Spatial Information Sciences **34** (4): 380–385.

Schumann, G., Bates, P.D., Horritt, M.S. & Matgen, P., 2009: Progress in integration of remote sensing-derived flood extent and stage data and hydraulic models. – Reviews of Geophysics **47**, RG4001.

Schumann, G., Matgen, P., Pappenberger, F., Black, A., Cutler, M., Hoffmann, L. & Pfister, L., 2006: The REFIX model: Remote Sensing based flood modelling". – International Archives of Photogrammetry, Remote Sensing and Spatial Information Sciences **36** (7): on CD.

Silveira, M. & Heleno, S., 2009: Separation between Water and Land using Region Based Level Sets. – IEEE Geoscience and Remote Sensing Letters **6** (3): 471–475.

Townsend, P.A., 2001: Mapping seasonal flooding in forested wetlands using multi-temporal radarsat SAR. – Photogrammetric Engineering and Remote Sensing **67** (7): 857–864.

UNU, 2010: United Nations University. – www.unu.edu/ (15th June 2010).

UN-SPIDER, 2010: United Nations Platform for Space-based Information for Disaster Management and Emergency Response. – www.un-spider.org/disaster/3665/2010-07-22/pakistan/flood-pakistan (6th September 2010).

Waisurasingha, C., Aniya, M., Hirano, A. & Sommut, W., 2008: Use of RADARSAT-1 data and digital elevation model to access flood damage and improve rice production in the lower part of the Chi River Basin, Thailand. – International Journal of Remote Sensing **29** (19–20): 5837–5850.

Zwenzner, H. & Voigt, S., 2009: Improved estimation of flood parameters by combining space based SAR data with very high resolution digital elevation data. – Hydrology and Earth System Sciences **13:** 567–576.

Addresses of the Authors:

Virginia Herrera Cruz & Dr. Marc Müller, Infoterra GmbH, D-88039 Friedrichshafen, Tel.: +49-7545-8-3382, -8439, e-mail: virginia.herrera@infoterra-global.com, marc.mueller@infoterra-global.com

Christian Weise, Definiens AG, D-80339 München, Trappentreustrasse 1, Tel.: +49-89-231180-0, e-mail: cweise@definiens.com